A Redetermination of the Neutrino Mass-Squared Difference in Tri-Maximal Mixing with Terrestrial Matter Effects

P. F. Harrison

Physics Department, Queen Mary and Westfield College
Mile End Rd. London E1 4NS. UK [1]

and

D. H. Perkins

Nuclear Physics Laboratory, University of Oxford
Keble Road, Oxford OX1 3RH. UK [2]

and

W. G. Scott

Rutherford Appleton Laboratory
Chilton, Didcot, Oxon OX11 0QX. UK [3]

Abstract

We re-fit for the neutrino mass-squared difference Δm^2 in the threefold maximal (ie. tri-maximal) mixing scenario using recent CHOOZ and SUPER-K data, taking account of matter effects in the Earth. While matter effects have little influence on reactor experiments and proposed long-baseline accelerator experiments with $L \lesssim 1000$ km, they are highly significant for atmospheric experiments, suppressing naturally ν_e mixing and enhancing $\nu_\mu - \nu_\tau$ mixing, so as to effectively remove the experimental distinction between threefold maximal and twofold maximal $\nu_\mu - \nu_\tau$ mixing. Threefold maximal mixing is fully consistent with the CHOOZ and SUPER-K data and the best-fit value for the neutrino mass-squared difference is $\Delta m^2 \simeq (0.98 \pm {0.30 \atop 0.23}) \times 10^{-3}$ eV^2.

To be published in Physics Letters B

---

[1]E-mail:p.f.harrison@qmw.ac.uk
[2]E-mail:d.perkins1@physics.oxford.ac.uk
[3]E-mail:w.g.scott@rl.ac.uk

1. Introduction

New limits on neutrino oscillations from the CHOOZ reactor experiment [1] definitively rule out threefold maximal lepton mixing with $\Delta m^2 \sim 10^{-2}$ eV^2 [2]. In the meantime however, the second-generation underground water-Cherenkov experiment SUPER-KAMIOKANDE [3] has superseded the older KAMIOKANDE experiment [4] as regards measurements of the atmospheric neutrino anomaly, with the latest experimental fits to $\nu_\mu - \nu_\tau$ mixing [5] clearly favouring a much smaller value of Δm^2 than before [6]. The aim of this paper is to underline the fact [7] that, in the light of such developments, threefold maximal mixing is *per se* far from excluded, in particular we emphasise, when terrestrial matter effects [8] are taken into account.

In this paper we re-fit for the neutrino mass-squared difference Δm^2 in the threefold maximal mixing scenario using the CHOOZ and SUPER-K data, taking full account of terrestrial matter effects which were hitherto neglected [2] [9] [10]. This simplest of all possible mixing schemes then continues to explain the great majority of oscillation data just as previously claimed, but now with $\Delta m^2 \sim 10^{-3}$ eV^2.

2. The Vacuum Scenario

In vacuum in the threefold maximal mixing scenario, the mixing matrix relating the neutrino flavour eigenstates ν_e, ν_μ, ν_τ to the neutrino mass eigenstates ν_1, ν_2, ν_3 (with masses $m_1 < m_2 < m_3$ respectively) takes the symmetric or 'democratic' form:

$$
\begin{array}{c}
\\
e \\
\mu \\
\tau
\end{array}
\begin{array}{ccc}
\nu_1 & \nu_2 & \nu_3
\end{array}
\left(
\begin{array}{ccc}
1/3 & 1/3 & 1/3 \\
1/3 & 1/3 & 1/3 \\
1/3 & 1/3 & 1/3
\end{array}
\right)
\tag{1}
$$

where here and throughout this paper we give directly the *squares* of the moduli of the mixing elements, in place of the mixing elements themselves. The mixing phenomenology is then completely determined by the two independent vacuum mass-squared differences $\Delta m^2 > \Delta m'^2$ (eg. $\Delta m^2 = m_3^2 - m_2^2$, $\Delta m'^2 = m_2^2 - m_1^2$). From the atmospheric data we have $\Delta m^2 \sim 10^{-3}$ eV^2 (see below) while from the solar data we found $\Delta m'^2 < 0.9 \times 10^{-11}$ eV^2 [2], so that in threefold maximal mixing, two masses are effectively degenerate and the spectrum of mass-squared differences is hierarchical.

Neutrino oscillations violate lepton flavour conservation and as a function of propagation length L the matrix of normalised transition amplitudes $A_{l'l}$ from a charged lepton state l to a charged lepton state l' is given directly by exponentiating the neutrino mass matrix squared $mm^\dagger$ ($\equiv m^2$) in the flavour basis: $A = \exp(-im^2L/2E)$,

where E is the energy of the neutrino, assumed to be relativistic. The mixing matrix U comprising the normalised eigenvectors of m^2 diagonalises the mass matrix thus: $U^\dagger m^2 U = \text{diag} (m_1^2, m_2^2, m_3^2)$. In terms of the mixing matrix the above matrix exponentiation is readily achieved by first exponentiating the diagonal matrix of phases and then rotating back to the flavour basis ('*un*-diagonalising') as follows: $A = U \, \text{diag} (e^{i\phi_1}, e^{i\phi_2}, e^{i\phi_3})U^\dagger$, where the phases $\phi_i = m_i^2 L/2E$ for $i = 1 \ldots 3$. Thus any transition amplitude $A_{l'l}$ may be written as the sum of three sub-amplitudes $A_{l'l}^{(i)} = X_{l'l}^{(i)} \, e^{i\phi_i}$, where $X_{l'l}^{(i)} = U_{l'i}U_{li}^*$, corresponding to the independent propagation of each of three neutrino mass eigenstates as usual. (Note that hypothetical 'sterile' neutrinos [11] play no role in the threefold maximal mixing scenario and are not considered here.)

Survival and appearance probabilities $P(l \to l) = |A_{ll}|^2$ and $P(l \to l') = |A_{l'l}|^2$ are then given by: $P(l \to l) = |A_{ll}^{(1)} + A_{ll}^{(2)} + A_{ll}^{(3)}|^2$ and $P(l \to l') = |A_{l'l}^{(1)} + A_{l'l}^{(2)} + A_{l'l}^{(3)}|^2$, respectively. In threefold maximal mixing the three sub-amplitudes corresponding to the three mass eigenstates are always of equal modulus $1/3$. All vacuum survival probabilities $P(l \to l)$ and appearance probabilities $P(l \to l')$, $P(l' \to l)$ are independent of flavour ($l, l' = e, \mu, \tau$). In the limit $\Delta m'^2 \to 0$ only one relative phase need be retained (eg. $\phi_3 - \phi_2$, where $\phi_2 = \phi_1$ for $\Delta m'^2 = 0$) and we are led to:

$$P(l \to l) = 5/9 + 4/9 \cos(\Delta m^2 L/2E) \tag{2}$$

and:

$$P(l \to l') = P(l' \to l) = 4/9 - 4/9 \cos(\Delta m^2 L/2E). \tag{3}$$

Averaging over a range of E (and/or L) such that oscillating terms no longer contribute, still in the limit $\Delta m'^2 \to 0$ with two sub-amplitudes adding 'coherently', one has for general mixing: $< P(l \to l) > = (X_{ll}^{(1)} + X_{ll}^{(2)})^2 + (X_{ll}^{(3)})^2$ where the $X_{ll}^{(i)}$ are real (the matrices $X^{(i)}$ are hermitian), and: $< P(l \to l') > = |X_{l'l}^{(1)} + X_{l'l}^{(2)}|^2 + |X_{l'l}^{(3)}|^2 = 2|X_{l'l}^{(3)}|^2$, where the last equality relies on unitarity ($X^1 + X^2 + X^3 = I$, the identity matrix). In the threefold scenario, one expects then a first 'step' or 'threshold' at $L \sim (\Delta m^2/2E)^{-1}$, marking the descent from $P(l \to l) = 1$ to:

$$< P(l \to l) > = (1/3 + 1/3)^2 + (1/3)^2 = 5/9 \tag{4}$$

and the rise from $P(l \to l') = P(l' \to l) = 0$ to:

$$< P(l \to l') > = < P(l' \to l) > = 2 \times (1/3)(1/3) = 2/9. \tag{5}$$

If $\Delta m'^2$ is non-zero there will be a second threshold at $L \sim (\Delta m'^2/2E)^{-1}$ beyond which all three sub-amplitudes add 'incoherently' so that: $< P(l \to l) > = (X_{ll}^{(1)})^2 + (X_{ll}^{(2)})^2 + (X_{ll}^{(3)})^2$ with: $< P(l \to l') > = |X_{l'l}^{(1)}|^2 + |X_{l'l}^{(2)}|^2 + |X_{l'l}^{(3)}|^2$, and in threefold maximal mixing: $< P(l \to l) > = < P(l \to l') > = < P(l' \to l) > = 1/3$.

3

For solar neutrinos, in the threefold maximal mixing scenario, matter effects in the Sun are expected to be rather unimportant [12] and the vacuum prediction Eq. (4) may be compared directly with the measured suppressions, at least for the gallium experiments. The same comparison for the SUPER-K [13] and HOMESTAKE [14] solar results, (correcting for the neutral current contribution to the $\nu e \rightarrow \nu e$ rate in SUPER-K) is limited by *de facto* uncertainties in the ^{8}B flux [9].

In the atmospheric experiments the initial beam comprises both ν_μ and ν_e, and account must be taken of $\nu_\mu \leftrightarrow \nu_e$ transitions, which tend to compensate the survival rates in Eq. (4). In the approximation that the flux ratio at production $\phi(\nu_\mu)/\phi(\nu_e) = 2/1$ the effective ν_μ suppression in vacuum becomes:

$$5/9 + 1/2 \times 2/9 = 2/3 \tag{6}$$

while the effective ν_e suppression becomes:

$$5/9 + 2 \times 2/9 = 1 \tag{7}$$

so that the ν_e rate is perfectly compensated in this case. The initial flux ratio is indeed $\phi(\nu_\mu)/\phi(\nu_e) \sim 2/1$ for $E \lesssim 1$ GeV (increasing with E thereafter).

While this concludes our discussion of the vacuum scenario, as we turn to consider the influence of matter effects it will prove useful to denote vacuum quantities with argument (0) for vacuum explicitly, thus we define: $m^2(0) \equiv m^2$, $U(0) \equiv U$, $\nu_i(0) \equiv \nu_i$, $m_i(0) \equiv m_i$, $\Delta m^2(0) \equiv \Delta m^2$, $\Delta m'^2(0) \equiv \Delta m'^2$ etc.

3. Terrestrial Matter Effects

In any scheme with ν_e mixing (eg. Eq. 1), matter effects in the Earth, in particular for atmospheric neutrinos, can be very significant indeed. Matter effects result from the forward scattering of ν_e from electrons in the matter, modifying the mass matrix by adding a term to the (e, e) entry of the vacuum mass matrix, proportional to the matter density ρ. Basic trends in matter phenomenology can usefully be anticipated by noting that in the limit of infinite density ($\rho \rightarrow \infty$), the ν_e becomes the heaviest neutrino, which being then itself a mass eigenstate, completely decouples in the mixing. In general clearly, before this limit is approached, masses, mixings etc. are functions of the matter density, hence we have: $m^2(\rho)$, $U(\rho)$, $\nu_i(\rho)$, $m_i(\rho)$, $\Delta m^2(\rho)$, $\Delta m'^2(\rho)$ etc., or more directly functions of the number density N_e of electrons in the matter.

In the present analysis matter effects are incorporated using the general 3×3 numerical program described in Ref. [12], where for a hierarchical spectrum $\Delta m^2(0) \gg \Delta m'^2(0)$, the formulae of Ref. [15] apply. Our numerical calculation proceeds in steps

4

$\Delta L = 100$ km through the Earth, with the density and composition of the Earth input as a function of depth from a recent tabulation [16]. Before giving our full numerical results in any detail however, in this section we sketch briefly the main trends predicted analytically in threefold maximal mixing with $\Delta m'^2(0) \ll \Delta m^2(0)$, as a function of increasing matter density, or equivalently as a function of increasing E.

We identify three significantly distinct density regimes where the mixing phenomenolgy remains essentially constant over a wide range of scales.

Firstly, clearly at very low matter densities $\sqrt{2}GN_e \ll \Delta m'^2(0)/E$ (where G is the Fermi constant) vacuum mixing remains essentially valid. Conceivably if $\Delta m'^2(0)$ is extremely small or zero ($\Delta m'^2 \lesssim 10^{-30}$ eV^2) this regime may not be realised in nature, even for neutrinos from distant supernovae propagating in deep space ($N_e \sim 10^3$ m^{-3}).

Next, at 'intermediate' densities ie. for $\Delta m'^2(0)/E \ll \sqrt{2}GN_e \ll \Delta m^2(0)/E$, matter effects lift the effective degeneracy between the two light neutrinos, such that in matter for neutrinos: $\nu_1(\rho) \to [\nu_1(0) - \nu_2(0)]/\sqrt{2}$ and $\nu_2(\rho) \to [\nu_1(0) + \nu_2(0)]/\sqrt{2}$ (up to phases), where the lighter matter mass eigenstate $\nu_1(\rho)$ has zero ν_e content. The mixing matrix is thereby deformed in matter as follows:

$$
\begin{array}{c}
\begin{array}{ccc} \nu_1(0) & \nu_2(0) & \nu_3(0) \end{array} \\
\begin{array}{c} e \\ \mu \\ \tau \end{array}
\left(\begin{array}{ccc} 1/3 & 1/3 & 1/3 \\ 1/3 & 1/3 & 1/3 \\ 1/3 & 1/3 & 1/3 \end{array} \right)
\end{array}
\longrightarrow
\begin{array}{c}
\begin{array}{ccc} \nu_1(\rho) & \nu_2(\rho) & \nu_3(\rho) \end{array} \\
\begin{array}{c} e \\ \mu \\ \tau \end{array}
\left(\begin{array}{ccc} . & 2/3 & 1/3 \\ 1/2 & 1/6 & 1/3 \\ 1/2 & 1/6 & 1/3 \end{array} \right)
\end{array}
\tag{8}
$$

with the smaller mass-squared difference $\Delta m'^2(\rho)/2E \to 2/3 \times \sqrt{2}GN_e$ in this case. The factor $2/3$ multiplying the matter mass scale reflects the fact that only two out of the three relevant 2×2 sub-determinants of the vacuum mass matrix are modified by the matter term. (Symmetrically, this same factor of $2/3$ will appear again multiplying the vacuum mass scale in the high density limit, see below). In the Earth's mantle ($\rho \sim 5$ g cm^{-3}) the matter mass-scale [17] is $\sqrt{2}GN_e \simeq 0.38 \times 10^{-3}$ eV^2/GeV, and the corresponding length-scale is $(\sqrt{2}GN_e)^{-1} \simeq 1040$ km/rdn. Thus the limit Eq. (8) should be physically relevant for atmospheric neutrinos, assuming $\Delta m^2(0) \sim 10^{-3}$ eV^2, for neutrino energies $E \lesssim 1$ GeV.

The matrix on the right-hand-side of Eq. (8) is one of the matrices with the ν_3 maximally mixed introduced in Ref. [9]. For $L \lesssim (\sqrt{2}GN_e)^{-1}$ the vacuum mixing predictions Eqs. (2)-(7) are reproduced. For $L \gtrsim (\sqrt{2}GN_e)^{-1}$, ie. beyond the 'matter threshold', the ν_μ survival probability averaged over E and L, is from row 2 of Eq. (8):

$$< P(\mu \to \mu) > = (1/2)^2 + (1/6)^2 + (1/3)^2 = 7/18 \tag{9}$$

while the average ν_e survival probability is (from row 1):

$$< P(e \to e) > = (0)^2 + (2/3)^2 + (1/3)^2 = 5/9 \tag{10}$$

5

just as it was after the first threshold, defined by Δm^2, in the vacuum analysis above. Likewise the corresponding $\nu_\mu \leftrightarrow \nu_e$ appearance probabilities are:

$$< P(\mu \to e) > = < P(e \to \mu) > = (0)(1/2) + (2/3)(1/6) + (1/3)(1/3) = 2/9 \quad (11)$$

(from rows 1 and 2) again as in the vacuum analysis.

For atmospheric neutrinos, in the approximation that the initial flux ratio $\phi(\nu_\mu)$ / $\phi(\nu_e) = 2/1$, the effective ν_μ suppression becomes:

$$7/18 + 1/2 \times 2/9 = 1/2 \quad (12)$$

replacing the vacuum prediction of $2/3$ from Eq. (6) [2][9][10], for $L \gg (\sqrt{2}GN_e)^{-1}$. The ν_e rate however remains perfectly compensated just as it was for $\phi(\nu_\mu)/\phi(\nu_e) = 2/1$ in the vacuum analysis and Eq. (7) applies. Note that these final suppression factors are exactly the same as would be expected in twofold maximal $\nu_\mu - \nu_\tau$ mixing.

Finally, for sufficiently high matter densities $\Delta m^2(0)/E \ll \sqrt{2}GN_e$ (or equivalently for sufficiently high neutrino energies), threefold maximal mixing tends physically to twofold maximal $\nu_\mu - \nu_\tau$ mixing with $\Delta m^2(0)$ fixing the smaller mass-squared difference $\Delta m'^2(\infty) \to 2/3 \times \Delta m^2(0)$ in matter, and with the larger matter mass-squared difference fixed by the matter mass-scale $\Delta m^2(\infty)/2E \to \sqrt{2}GN_e$:

$$
\begin{array}{c}
\begin{array}{ccc}
\nu_1(\rho) & \nu_2(\rho) & \nu_3(\rho)
\end{array} \\
\begin{array}{c}
e \\ \mu \\ \tau
\end{array}
\left(
\begin{array}{ccc}
. & 2/3 & 1/3 \\
1/2 & 1/6 & 1/3 \\
1/2 & 1/6 & 1/3
\end{array}
\right)
\end{array}
\longrightarrow
\begin{array}{c}
\begin{array}{ccc}
\nu_1(\infty) & \nu_2(\infty) & \nu_3(\infty)
\end{array} \\
\begin{array}{c}
e \\ \mu \\ \tau
\end{array}
\left(
\begin{array}{ccc}
. & . & 1 \\
1/2 & 1/2 & . \\
1/2 & 1/2 & .
\end{array}
\right)
\end{array}. \quad (13)
$$

As foreseen, with the matter interaction affecting ν_e directly, $\nu_e \to \nu_3$ asymptotically. Thus the higher frequency oscillations have zero amplitude whereby, for example, the ν_τ appearance probability in a high energy ν_μ beam becomes simply:

$$P(\mu \to \tau) = 1/2 - 1/2 \cos[2/3 \times \Delta m^2(0)L/2E]. \quad (14)$$

For $L \to 0$ vacuum predictions must always be reproduced [8]. Clearly Eq. (14) coincides with Eq. (3) for $L \to 0$. For $L \to \infty$ we have $< P(\mu \to \tau) > \to 1/2$, so that ν_τ appearance may be said to be enhanced by matter effects, cf. Eq. (5), and correspondingly $< P(\mu \to \mu) > \to 1/2$ in that case. As the ν_e decouples completely $P(e \to e) \to 1$ with $P(\mu \to e) = P(e \to \mu) \to 0$ in the limit, so that in the atmospheric experiments there are no significant compensation effects expected at the highest energies, despite the fact that the production flux ratio $\phi(\nu_\mu)/\phi(\nu_e)$ is becoming large, $\phi(\nu_\mu)/\phi(\nu_e) \gtrsim 3/1$ for $E \gtrsim 10$ GeV.

The important conclusion is that threefold maximal mixing with terrestrial matter effects *exactly* mimics twofold $\nu_\mu - \nu_\tau$ mixing for the atmospheric neutrino rates

both at the lowest energies and at the highest energies, but for somewhat different reasons in the two cases, as we have seen. Observable differences between threefold and twofold mixing are expected at best only in a window of 'intermediate' energies, where $\phi(\nu_\mu)/\phi(\nu_e) > 2/1$ but before the limit Eq. (13) is approached. Of course our numerical results reported below incorporate the full expected energy and zenith-angle dependence of the flux ratio at production $\phi(\nu_\mu)/\phi(\nu_e)$ [18], with appropriate averaging over detailed $\nu/\bar{\nu}$ differences, neglected in the above discussion.

4. Multi-GeV Zenith-Angle Distributions

When oscillations are not individually resolved the neutrino mass-squared difference is determined by the location of the corresponding threshold on the L/E scale (the location of the 'matter threshold' is of course energy-independent, and is arguably better studied as a function of L rather than L/E). For atmospheric neutrinos the neutrino flight-path L is related to the zenith angle θ of the neutrino by

$$L = \sqrt{R_\oplus^2 \cos^2\theta + 2R_\oplus H + H^2} - R_\oplus \cos\theta \tag{15}$$

where $R_\oplus \simeq 6380$ km is the radius of the Earth and $H \sim 20$ km is the effective height of the atmosphere. In the water-Cherenkov experiments the neutrino zenith angle is estimated using the measurement of the outgoing charged-lepton, which will best correlate with the neutrino direction at higher energies, so that we expect the most reliable information to come from the so-called multi-GeV sample (ie. events with charged lepton momentum $p \gtrsim 1.3$ GeV for electrons and $p \gtrsim 1.4$ GeV for muons).

Fig. 1 shows the measured zenith angle distributions for multi-GeV events, combining the SUPER-K [5] and KAMIOKA [6] data for maximum statististical weight. There is clear evidence for a step (or 'threshold') as a function of $\cos\theta$ with an approximate 50% suppression of the μ-like events for $\cos\theta < -0.2$. At the same time no such effect is apparent in the corresponding distribution for e-like events, Fig. 1b. Since a full monte-carlo simulation including detector effects etc. is beyond the scope of the present paper, we have wherever possible in this analysis made appropriate use of the expected event rates for no oscillations given by the experimenters themselves. Thus in Fig. 1 we plot the ratio of observed to expected events in preference to the event rates themselves, in order to minimise dependence on detector acceptance etc. The plotted ratio in each case is normalised to the threefold maximal prediction with matter effects for $\Delta m^2 = 0.98 \times 10^{-3}$ eV^2 (which is the overall best-fit Δm^2 in threefold maximal mixing, see Section 5 below) so that it is only the shape of the zenith-angle dependence which is being tested here, with no reliance on absolute fluxes.

In Fig. 1 the solid curves represent the threefold maximal mixing predictions computed taking full account of terrestrial matter effects and compensation effects for $\Delta m^2 = 0.98 \times 10^{-3}$ eV^2, with the dotted curves showing the corresponding vacuum predictions. The dashed curves represent twofold maximal $\nu_\mu - \nu_\tau$ mixing for the same value of Δm^2. All the above curves are averaged over the multi-GeV energy distribution and incorporate angular smearing. We take gaussian smearing in angle around the neutrino direction with a width fixed from existing $\nu/\bar{\nu}$ data [21], where the width falls with energy proportional to $1/\sqrt{E}$. The mean angle between the neutrino direction and the charged-lepton direction is then 21° for the multi-GeV sample (and 43° for subGeV events with $p > 400$ MeV/c, see Section 5 below). For comparison, angular smearing resulting from the Cherenkov method itself has the same energy dependence, but is an order of magnitude smaller [19] and may be neglected. Particle mis-identification effects, ie. mis-classification of μ-events as e-events and vice versa, believed to become important only at the percent level [20], are also neglected in our analysis. As is clear from Fig. 1 (and see also Table 1, Section 5 below) both threefold maximal mixing with matter effects and twofold maximal $\nu_\mu - \nu_\tau$ mixing are consistent with the measured multi-GeV zenith-angle distributions.

The predicted up/down ratios $(U/D)_\mu$ and $(U/D)_e$ for multi-GeV μ-like and e-like events respectively, are shown in Fig. 2, as functions of Δm^2, for each of the various mixing scenarios above. The up/down ratios are defined from Fig. 1 as the ratio of up to down rates with $|\cos\theta| > 0.2$ and are expected [22] to be relatively free of systematic effects, eg. flux uncertainties. At multi-GeV energies the initial flux ratio $\phi(\nu_\mu)/\phi(\nu_e) > 2/1$, and in the case of threefold maximal mixing one expects to see *over*-compensation of the ν_e rate, ie. $(U/D)_e > 1$, cf. Eq. (7), and *under*-compensation of the ν_μ rate, ie. $(U/D)_\mu < 1/2$, cf. Eq. (12) (with smearing $(U/D)_\mu \simeq 1/2$, Fig. 2), at least for $\Delta m^2 \gtrsim 10^{-3}$ eV^2. As is clear from Fig. 2, for $\Delta m^2 \lesssim 10^{-3}$ eV^2 over-compensation of the ν_e rate is suppressed relative to the vacuum prediction as a result of terrestrial matter effects, with $(U/D)_e$ approaching unity as $\Delta m^2 \to 0$, simulating $\nu_\mu - \nu_\tau$ mixing as discussed above.

In Fig. 2 the data points with error bars represent the measured up/down ratios based on the combined SUPER-K and KAMIOKA data: $(U/D)_\mu = 0.53 \pm \begin{smallmatrix} 0.05 \\ 0.04 \end{smallmatrix}$ and $(U/D)_e = 0.99 \pm \begin{smallmatrix} 0.11 \\ 0.10 \end{smallmatrix}$, these being plotted arbitrarily at $\Delta m^2 \sim 0.98 \times 10^{-3}$ eV^2, and extended by the shaded bands. The up/down ratio for all events $(U/D)_{e+\mu} = 0.68 \pm 0.05$ (not shown) is less incisive, but has the advantage of being independent of particle misidentifiaction effects. Clearly the data on the up/down ratios are consistent with either twofold maximal $\nu_\mu - \nu_\tau$ mixing, or with threefold maximal mixing with inclusion of terrestrial matter effects, for $\Delta m^2 \sim 10^{-3}$ eV^2.

5. The Sub-GeV Data, R-values and Upward Muons

The KAMIOKA/SUPER-K collaborations have also given zenith angle distributions for sub-GeV events (lepton momentum $p < 1.3$ GeV), as well as values for the double ratio $R = (\mu/e)_{DATA}/(\mu/e)_{MC}$ for sub-GeV and multi-GeV events, and independent data on upward muons. For some of these data-sets there are significant systematic effects to be considered, against the gain in statistiscal weight.

Fig. 3 shows the observed zenith angle dependence for the higher energy ($p > 400$ MeV) subset of the sub-GeV sample in the SUPER-K experiment. The dashed curve is the prediction of threefold maximal mixing for $\Delta m^2 \simeq 0.98 \times 10^{-3}$ eV^2 including terrestrial matter effects and compensation effects, showing clearly the 'matter threshold' and the matter-induced oscillations, but neglecting angular smearing. The solid curve includes the expected effect of angular smearing as discussed previously, and which is now very significant. A fit to the data of Fig. 3 in threefold or twofold mixing yields a best-fit $\Delta m^2 \sim 2 \times 10^{-3}$ eV^2 (χ^2/DOF $\simeq 5.0/7$, CL$\simeq 66\%$). The zenith-angle data for the lower energy ($p < 400$ MeV) subset of the sub-GeV data are not included in this analysis. Angular smearing and geomagnetic effects [23] are expected to dominate the zenith-angle dependence at such low energies, where very little zenith-angle dependence is seen and essentially no Δm^2 information survives.

The integrated ratio of ratios $R = (\mu/e)_{DATA}/(\mu/e)_{MC}$ is independent of smearing effects, but dependent on flux uncertainties which affect the flavour ratio $\phi(\nu_\mu)/\phi(\nu_e)$, particularly since e-like and μ-like events have different Cherenkov thresholds. The latest R-values given by the SUPER-K experiment are: $R = 0.67 \pm 0.02 \pm 0.05$ for the sub-GeV sample and $R = 0.66 \pm 0.04 \pm 0.08$ for the multi-GeV sample, where the first error is statistical and the second is the systematic error in each case, as given by SUPER-K. These results are shown in Fig. 4 by the data points and shaded bands, together with the predictions from threefold maximal mixing (solid curves) and twofold $\nu_\mu - \nu_\tau$ mixing (dashed curves), plotted as a function of Δm^2. Clearly within the combined statistical and systematic errors the consistency with $\Delta m^2 \sim 10^{-3}$ eV^2 is perfectly acceptable. It is perhaps worth commenting here that threefold maximal mixing goes some way to resolving the problem of the near-equality of the multi-GeV and sub-GeV R-values raised by LoSecco [24].

In the underground detectors upward muons result from neutrino interactions in the rock surrounding the detector [25] [26]. Fig. 5 shows the double ratio S of stopping to through muons for data divided by monte-carlo: $S = 0.59 \pm 0.06 \pm 0.08$ as measured by SUPER-K [27] (data point and shaded band). The solid curve is our threefold

9

maximal mixing prediction with terrestrial matter effects included, plotted as a function of Δm^2, while the dashed curve corresponds to twofold maximal $\nu_\mu - \nu_\tau$ mixing. The shift of a factor of 2/3 in Δm^2 between the two curves as expected at high energies, see Eq. (14), is apparent, with threefold maximal mixing showing a slightly lower minimum value for S, due to terrestrial matter effects. The relatively low measured value of S seems to point here to $\Delta m^2 \sim 10^{-3}$ eV^2 in either threefold or twofold mixing.

6. The CHOOZ Data and Overall Fit

The CHOOZ experiment [1] measures the survival probability $P(\bar{e} \rightarrow \bar{e})$ for $\bar{\nu}_e$ by comparing the observed to expected rates for the reaction $\bar{\nu}_e + p \rightarrow e^+ + n$ at a distance $L \sim 1$ km from the CHOOZ reactor site. The initial result for $P(\bar{e} \rightarrow \bar{e})$ is shown in Fig. 6, plotted as a function of antineutrino energy E, related to the measured positron energy E_e by $E = 1.8 + E_e$ MeV. The data so far are consistent with $P(\bar{e} \rightarrow \bar{e}) = 1$, and no oscillation signal is claimed.

At such short pathlengths $L \ll (\sqrt{2}GN_e)^{-1}$, matter effects can be safely neglected, and in Fig. 6 the solid curve is the threefold maximal mixing prediction calculated from the vacuum formula Eq. (2) for $\Delta m^2 = 0.98 \times 10^{-3}$ eV^2. Twofold maximal $\nu_\mu - \nu_\tau$ mixing predicts $P(\bar{e} \rightarrow \bar{e}) = 1$ as shown by the dashed line, independent of matter effects and independent of E (and Δm^2). The best-fit to the data of Fig. 6 in threefold maximal mixing is: $\Delta m^2 = 0.60 \times 10^{-3}$ eV^2 ($\chi^2/\text{DOF} = 10.6/9$, CL= 30%), although clearly the data are also fully consistent with $\Delta m^2 \rightarrow 0$, ($\chi^2/\text{DOF} \rightarrow 11.0/9$, CL= 28%), or equivalently with $\nu_\mu - \nu_\tau$ mixing.

Our overall fit for the neutrino mass-squared difference Δm^2 is based on the atmospheric data already discussed, taken together with the CHOOZ data for $P(\bar{e} \rightarrow \bar{e})$ as a function of E. Specifically we compute the total χ^2 summed over all the bins displayed in Figs. 1, 3, 4, 5, 6 as a function of Δm^2 for twofold maximal $\nu_\mu - \nu_\tau$ mixing and for threefold maximal mixing with matter effects. There are 33 data points in total, but 4 normalisation factors to be determined in each case (one for each zenith-angle plot) in addition to Δm^2, so that there are $33 - 5 = 28$ DOF in each fit.

The results of the overall fits are shown in Fig. 7. For twofold maximal $\nu_\mu - \nu_\tau$ mixing (dashed curve) there is a broad minimum in χ^2 extending over the range $\Delta m^2 \sim 7 \times 10^{-4} - 4 \times 10^{-3}$ eV^2 with the best-fit $\Delta m^2 \sim 2.2 \times 10^{-3}$ eV^2 corresponding to an excellent fit ($\chi^2/\text{DOF} = 18.7/28$, CL = 91%). For threefold maximal mixing (solid curve) the mass-squared difference is highly constrained by the CHOOZ data giving a much narrower minimum in χ^2, and a significantly more restricted Δm^2-range: $\Delta m^2 \simeq (0.98 \pm^{0.30}_{0.23}) \times 10^{-3}$ eV^2, however still corresponding to a very good

fit ($\chi^2/\text{DOF} = 25.4/28$, CL $= 61\%$). A full breakdown of the χ^2-contributions coming from the various data-sets is given in Table 1.

While both threefold maximal mixing and twofold maximal $\nu_\mu - \nu_\tau$ mixing are consistent with the combined data then, it is clear that in threefold maximal mixing the best-fit value of Δm^2 is extremely close to the published CHOOZ limit [1] on Δm^2 computed for the case of twofold maximal $\nu_\mu - \nu_e$ mixing. This near-coincidence of the best-fit value with the published upper-limit strongly suggests that if threefold maximal mixing is valid, either of the two existing long-baseline reactor experiments CHOOZ [1] or PALO-VERDE [28] could, with continued running, increased detector mass and especially with increased baseline $L \sim 5 - 10$ km, still be the first experiments to observe 'man-made' neutrino oscillations, and to establish the existence of ν_e mixing at the 'atmospheric scale' $\Delta m^2 \sim 10^{-3}$ eV^2. Otherwise the KAMLAND experiment [29] should be decisive.

7. Perspective and Future Prospects

Naturally there are many other mixing schemes which can similarly describe the data. We mention explicitly here the Fritzsch-Xing hypothesis [30], and in particular also the 'bi-maximal' hypothesis [31] and its generalisations [32] [33] in which the ν_3 is assumed to have ν_e, ν_μ, ν_τ content $0, 1/2, 1/2$ perfectly replicating the phenomenology of twofold $\nu_\mu - \nu_\tau$ mixing as far as the atmospheric experiments are concerned. In such schemes the zero or near-zero in the top right-hand corner of the mixing matrix guarantees no ν_e mixing at the atmospheric scale $\Delta m^2 \sim 10^{-3}$ eV^2.

Clearly certain 'bi-maximal' schemes can mimic 'tri-maximal' mixing (ie. threefold maximal mixing) extremely effectively. For example a bi-maximal scheme with the ν_2 (tri-) maximally mixed (ie. having ν_e, ν_μ, ν_τ content 1/3, 1/3, 1/3), would have very similar phenomenology to threefold maximal mixing even for the solar data, with $P(e \to e) = 5/9$ in the gallium experiments and with the added possibility to exploit a large angle MSW solution with $P(e \to e) = 1/3$ in the 'bathtub', in the higher energy experiments, for some particular $\Delta m'^2 \sim 10^{-5}$ eV^2. We emphasise however that in the threefold maximal mixing scenario suppression of ν_e mixing at the atmospheric scale $\Delta m^2 \sim 10^{-3}$ eV^2, occurs *naturally* as a result of terrestrial matter effects without the insertion of an arbitrary zero in the mixing matrix as in the bi-maximal schemes.

As regards 'bi-maximal' versus 'tri-maximal' mixing then, the crucial experimental question would seem to be whether or not there is appreciable vacuum ν_e mixing at the atmospheric scale. This question might perhaps be answered in the future by the SUPER-K experiment itself, with the observation of a significant upward excess

of e-like events in the atmospheric data at multi-GeV energies. The predicted U/D ratio for ν_e in threefold maximal mixing, when matter effects are included, peaks as a function of neutrino energy at $E \sim 7$ GeV, where $(U/D)_e \simeq 1.13$.

Together with reactor experiments, long-baseline accelerator experiments using high-energy ν_μ-beams will also probe ν_e mixing. Fig. 8 shows the predicted energy-averaged appearance probability $< P(\mu \to e) >$ for various mean neutrino energies in threefold maximal mixing for $\Delta m^2 = 1.0 \times 10^{-3}$ eV^2. The curves are calculated with and without matter effects (solid and dotted curves respectively) and for visual clarity are shown averaged $(50 : 50)$ over $\nu/\bar{\nu}$ beams. The suppression of ν_e appearance as a result of matter effects is plainly visible at large L, but for all proposed experiments with $L \lesssim 1000$ km, matter effects can be largely neglected.

8. Conclusion

In this paper we have shown that the recent data from CHOOZ and SUPER-K are consistent with threefold maximal mixing (ie. 'tri-maximal' mixing) for a neutrino mass-squared difference $\Delta m^2 \simeq (0.98 \pm {}^{0.30}_{0.23}) \times 10^{-3}$ eV^2. With just a very few acknowledged exceptions, notably the LSND appearance result [34] and possibly also the HOMESTAKE solar measurement [14], the totality of previous data are also known [9] to be in good agreement with this hypothesis [2].

Assuming tri-maximal mixing therefore, and taking a hierarchical spectrum of neutrino masses similar to that of the quarks and leptons, we have for the heavy neutrino mass $m_3 \sim 30 \pm 5$ meV. This result is consistent with a 'see-saw' relation to the up-type quarks for a heavy (right-handed) Majorana mass $M_R \sim 1.0 \times 10^{15}$ GeV. The compton wavelenth of the heavy neutrino ν_3 is $\lambda_3 \sim 1/20$ mm. Such a neutrino would make little contribution to cosmological dark matter.

References

[1] M. Apollonio et al. Phys. Lett. B 420 (1998) 397. (hep-ex/9711002).

[2] P. F. Harrison, D. H. Perkins and W. G. Scott. Phys. Lett. B 349 (1995) 357.

[3] Y. Fukuda et al. Phys. Lett. 436 (1998) 33 (hep-ex/9805006).
    Y. Fukuda et al. Phys. Lett. 433 (1998) 9 (hep-ex/9803006).

[4] K. S. Hirata et al. Phys. Lett. B 205 (1988) 416; B280 (1992) 146.
    Y. Suzuki. ICHEP '96. ed. Z. Ajduk and A. K. Wroblewski. (1997).

[5] Y. Fukuda et al. Phys. Rev. Lett. 81 (1998) 1562 (hep-ex/9807003).
    M. Messier. APS Division of Particles and Fields, UCLA (1999).

[6] Y. Fukuda et al. Phys. Lett. B335 (1994) 237.

[7] R. Foot, R. R. Volkas and O. Yasuda. Phys. Lett. B 433 (1998) 82.

[8] V. Barger et al. Phys. Rev. D22 (1980) 2718.
    J. Pantaleone. Phys. Rev. D49 (1994) 2152; hep-ph/9810467.
    G. L. Fogli et al. Phys. Rev. D 59 (1999) 033.001.

[9] P. F. Harrison, D. H. Perkins and W. G. Scott. Phys. Lett. B 396 (1997) 186.

[10] W. G. Scott. Nucl. Phys. B (Proc. Suppl.) 66 (1998) 411.

[11] D. O. Caldwell and R. N. Mohapatra. Phys. Rev. D 48 (1993) 3269.
     J. Peltoniemi and J. W. Valle. Nucl. Phys. B 408 (1993) 406.

[12] P. F. Harrison, D. H. Perkins and W. G. Scott. Phys. Lett. B 374 (1996) 111.

[13] Y. Fukuda et al. Phys. Rev. Lett. 81 (1998) 1158;4279 (hep-ex/9805021).

[14] B. T. Cleveland et al. Nucl. Phys. B (Proc. Suppl.) 38 (1995) 47.

[15] C. Giunti, C. W. Kim and M. Monteno. Nucl. Phys. B521 (1998) 3.

[16] J. A. Jacobs. The Earth's core. Academic Press (1987).
     A. M. Dziewonski and D. L. Anderson. Phys. Earth Planet Int. 25 (1981) 297.

[17] L. Wolfenstein. Phys. Rev. D17 (1978) 2369; D20 (1979) 2634.
     R. R. Lewis. Phys. Rev. D21 (1980) 663.
     P. Langacker. et al. Phys. Rev. D27 (1983) 1228.

[18] D. H. Perkins. Nucl. Phys. B399 (1993) 3.

[19] M. Nakahata et al. Nucl. Instrum. Methods. A421 (1999) 113. hep-ex/980727.

[20] S. Kasuga et al. Phys. Lett. B 374 (1996) 238.

[21] T. Eichten et al. Phys. Lett. B 40 (1973) 281.
W. G. Scott. D. Phil. Thesis. Oxford (1975).

[22] R. Foot, R. R. Volkas and O. Yasuda. Phys. Lett. B 421 (1998) 245.

[23] P. Lipari, T. Stanev and T. K. Gaisser. Phys. Rev. D 58 (1998) 073003.
T. K. Gaisser. New Era in Neutrino Physics. Tokyo (1998) hep-ph/9811314.

[24] J. M. LoSecco. hep-ph/9807359.

[25] M. Ambrosio et al. Phys. Lett. B434 (1998) 451 (hep-ex/9807005).

[26] T. Hatakeyama et al. Phys. Rev. Lett. 81 (1998) 2016 (hep-ex/9806038).

[27] Y. Fukuda et al. hep-ex/9812014. T. Kajita. hep-ex/9810001.
Y. Suzuki. WIN99 Capetown (1999).

[28] F. Boehm. VIII International Workshop on Neutrino Telescopes. Venice. (1999).

[29] T. Alivisatos et al. Stanford-HEP-98-03;Tohoku-RCNS-98-15. (1998).

[30] H. Fritzsch and Z. Xing. Phys. lett. B 372 (1996) 265; B 440 (1998) 313.

[31] V. Barger et al. Phys. Lett. B437 (1998) 107.
A. J. Bahz, A. S. Goldhaber and M. Goldhaber. Phys. Rev. Lett. 81 (1998) 5730.
D. V. Ahluwalla. Mod. Phys. Lett. A 18 (1998) 2249.
H. Giorgi and S. L. Glashow. hep-ph/9808293.
W. G. Scott. IDM98 Buxton (1998). RAL-TR-1998-072.

[32] G. Altarelli and F. Feruglo. Phys. Lett. B439 (1998) 112; JHEP 9811:021 (1998).

[33] R. N. Mohapatra and S. Nussinov. hep-ph/9809415.
C. Giunti. hep-ph/9810272.
C. Jarlskog et al. hep-ph/9812282.
R. Barbieri et al. hep-ph/9901228.
S. Lola and G. G. Ross. hep-ph/9902283.

[34] C. Athanassopoulos et al. Phys. Rev. Lett. 75 (1995) 2650; 81 (1998) 1774.
Phys. Rev. C 54 (1996) 2685.

.

	3-Fold Max. (mat.) $\Delta m^2 = 0.98 \times 10^{-3}$ eV^2	2-Fold Max. $(\nu_\mu - \nu_\tau)$ $\Delta m^2 = 2.2 \times 10^{-3}$ eV^2
Zenith-Angle Multi-GeV	$\chi^2/\text{DOF} = 6.5/7$ (CL = 48%)	$\chi^2/\text{DOF} = 2.0/7$ (CL = 96%)
+ Zenith-Angle Sub-GeV	$\chi^2/\text{DOF} = 11.9/15$ (CL = 69%)	$\chi^2/\text{DOF} = 7.1/15$ (CL = 95%)
+ R-Values Mult+Sub	$\chi^2/\text{DOF} = 13.2/17$ (CL = 72%)	$\chi^2/\text{DOF} = 7.6/17$ (CL = 97%)
+ Upward-Muons Stop/Thru	$\chi^2/\text{DOF} = 13.6/18$ (CL = 75%)	$\chi^2/\text{DOF} = 7.7/18$ (CL = 98%)
+ CHOOZ $P(\bar{e} \to \bar{e})$	$\chi^2/\text{DOF} = 25.4/28$ (CL = 61%)	$\chi^2/\text{DOF} = 18.7/28$ (CL = 91%)

Table 1: Cumulative breakdown of χ^2 contributions and confidence levels for the various data-sets (see text) calculated for threefold maximal mixing with $\Delta m^2 = 0.98 \times 10^{-3}$ eV^2 and twofold maximal $\nu_\mu - \nu_\tau$ mixing with $\Delta m^2 = 2.2 \times 10^{-3}$ eV^2. The Δm^2 values quoted correspond to the overall χ^2-minimum in each case summed over all the data-sets listed. Both threefold maximal mixing and twofold maximal $\nu_\mu - \nu_\tau$ mixing give excellent overall fits to the data.

Figure Captions

Figure 1. a) The combined KAMIOKA/SUPER-K multi-GeV zenith angle distribution for a) μ-like events and b) e-like events. The solid curve in each case is the threefold maximal mixing prediction for $\Delta m^2 = 0.98 \times 10^{-3}$ eV^2, including terrestrial matter effects and compensation effects. The twofold maximal $\nu_\mu - \nu_\tau$ mixing predictions (dashed curve) and the threefold vacuum predictions (dotted curve) are also shown. Either threefold maximal mixing with matter effects or twofold maximal $\nu_\mu - \nu_\tau$ mixing are consistent with the multi-GeV zenith-angle data.

Figure 2. The combined KAMIOKA/SUPER-K data on the up/down ratios for e-like and μ-like events with $|\cos\theta| > 0.2$ (data-points and shaded bands). The various theoretical predictions are plotted versus Δm^2. Threefold maximal mixing with matter effects (solid curves) approaches two-fold maximal $\nu_\mu - \nu_\tau$ mixing (dashed curves) as $\Delta m^2 \to 0$, and over-compensation of the ν_e-rate (expected in vacuum, dotted curve) is suppressed, consistent with the data.

Figure 3. The SUPER-K sub-GeV zenith angle distributions (lepton momentum $p > 400$ MeV) for a) μ-like and b) e-like events. The curves correspond to threefold maximal mixing with terrestrial matter effects and compensation effects for $\Delta m^2 = 0.98 \times 10^{-3}$ eV^2. The dashed curve shows the expected energy-independent 'matter oscillations' of amplitude $\pm 1/6$ and density-dependent wavelength, which are obscured by angular smearing (solid curve) in the water-Cherenkov experiments.

Figure 4. The atmospheric neutrino ratio $R = (\mu/e)_{DATA}/(\mu/e)_{MC}$ as measured by SUPER-K (data-points and shaded bands). Within the statistical and systematic errors shown the data for R are consistent with $\Delta m^2 \sim 10^{-3}$ eV^2. Threefold maximal mixing including terrestrial matter effects (solid curves) predicts less change in $< R >$ from sub-GeV to multi-GeV energies (open and filled data points respectively) than twofold maximal $\nu_\mu - \nu_\tau$ mixing (dashed curves).

Figure 5. The double ratio S of stopping to through muons in data and monte-carlo in SUPER-K (data point and shaded band). Threefold maximal mixing with matter effects included (solid curve) predicts a somewhat lower minimal suppression, but is otherwise very similar to the twofold maximal $\nu_\mu - \nu_\tau$ mixing prediction (dashed curve), with the shift of a factor 2/3 on the Δm^2-scale, see Eq. (14). The data for S point to $\Delta m^2 \sim 10^{-3}$ eV^2 in both twofold and threefold mixing.

Figure 6. The data from the CHOOZ reactor experiment on the $\bar{\nu}_e$ survival probability $P(\bar{e} \to \bar{e})$ plotted as a function of neutrino energy $E = 1.8 + E_e$ where E_e is the measured positron energy. The solid curve shows the threefold maximal mixing prediction for $\Delta m^2 = 0.98 \times 10^{-3}$ eV^2. With continued running, increased detector mass and particularly with increased baseline $L \sim 5 - 10$ km, significant $\bar{\nu}_e$ disappearance might well be established in reactor experiments.

Figure 7. The overall χ^2 in our combined fit, plotted versus Δm^2. In twofold maximal $\nu_\mu - \nu_\tau$ mixing (dashed curve) there is a broad minimum extending over the range $\Delta m^2 \sim 7 \times 10^{-4} - 4 \times 10^{-3}$ eV^2 with a best-fit $\Delta m^2 \simeq 2.2 \times 10^{-3}$ eV^2 corresponding to an excellent fit ($\chi^2/\mathrm{DOF} = 18.7/28$, CL = 91%). In threefold maximal mixing (solid curve) Δm^2 is relatively precisely determined: $\Delta m^2 \simeq (0.98 \pm^{0.30}_{0.23}) \times 10^{-3}$ eV^2, but still corresponds to a very good fit ($\chi^2/\mathrm{DOF} = 25.4/28$, CL = 61%).

Figure 8. Suppression of ν_e mixing by terrestrial matter effects. The predicted ν_e appearance probability as a function of the propagation length L through the Earth, in threefold maximal mixing with $\Delta m^2 \equiv 10^{-3}$ eV^2. The dotted curve is for vacuum mixing only and the solid curve includes matter effects (for visual clarity the curves plotted refer to a $50 : 50$ average over $\nu/\bar{\nu}$ beams). Matter oscillations, with reduced wavelength $(\sqrt{2}GN_e)^{-1}$, are evident at large L, but proposed long-baseline accelerator experiments with $L \lesssim 1000$ km are largely unaffected.
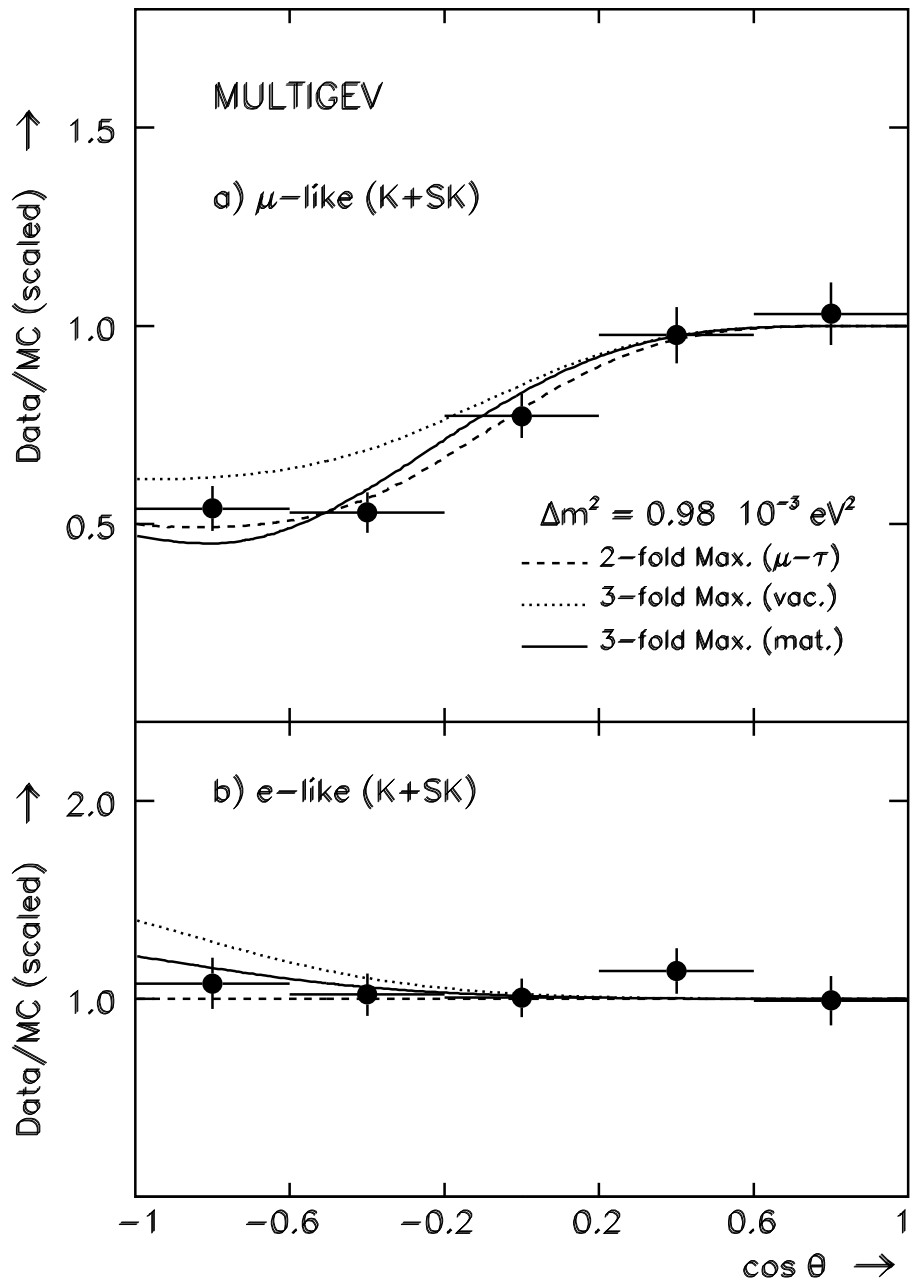
Figure 1

Figure 2
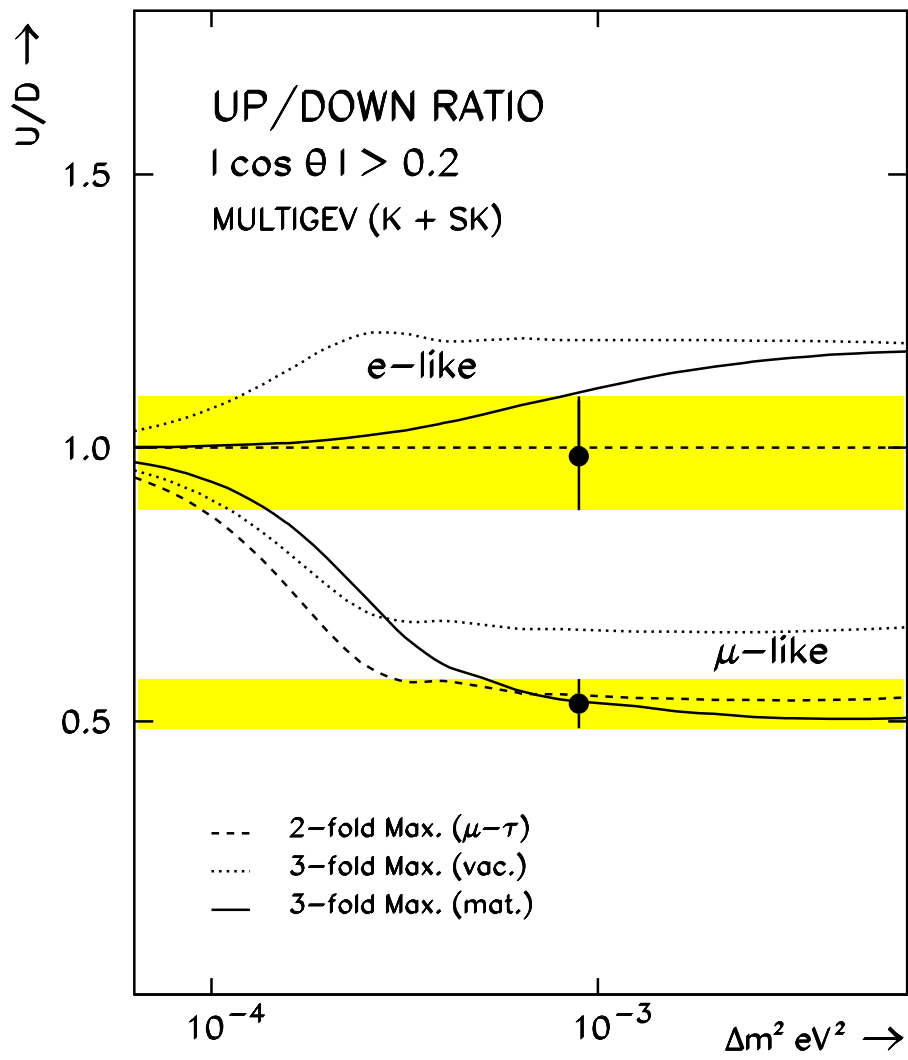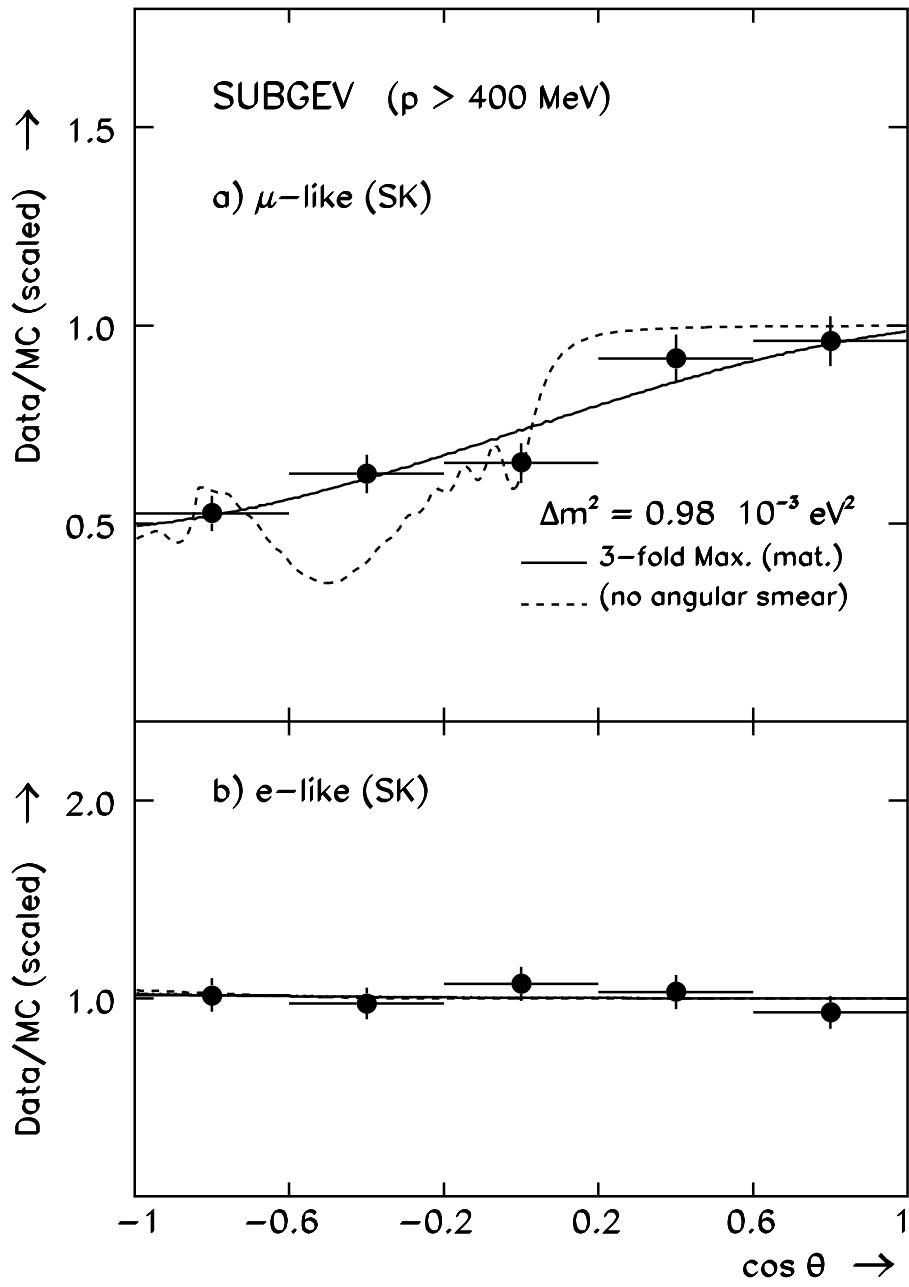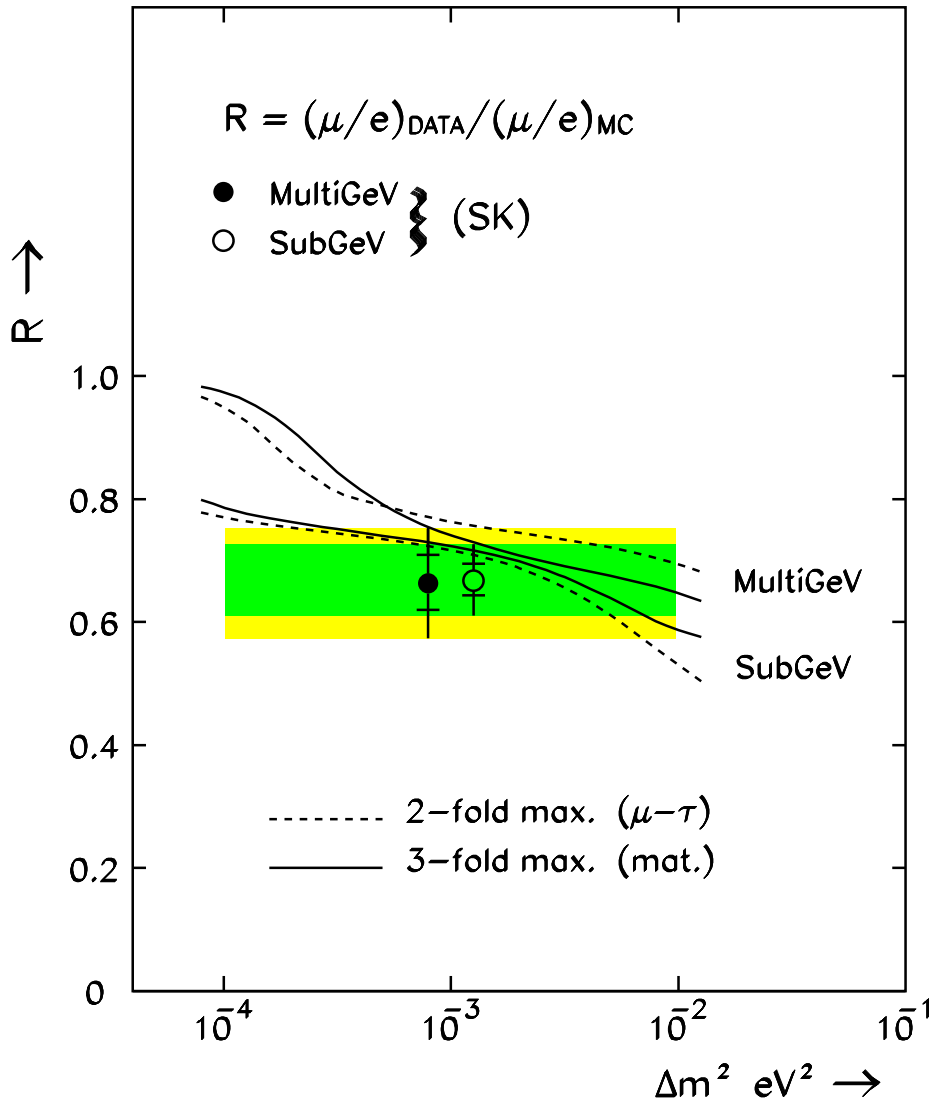
SUBGEV (p > 400 MeV)

a) μ−like (SK)

$\Delta m^2 = 0.98 \ \ 10^{-3} \ eV^2$

——— 3−fold Max. (mat.)

- - - - (no angular smear)

b) e−like (SK)

$\cos \theta \ \rightarrow$

Data/MC (scaled)

Figure 3

R = $(\mu/e)_{DATA}/(\mu/e)_{MC}$

● MultiGeV
○ SubGeV } (SK)

R →

MultiGeV

SubGeV

---- 2-fold max. $(\mu-\tau)$
—— 3-fold max. (mat.)

Δm^2 eV² →

Figure 4

Figure 5

CHOOZ REACTOR DATA

$P(\bar{e} \to \bar{e})$

$\Delta m^2 = 0.98 \ 10^{-3} \ eV^2$

- - - - - 2-fold Max. $(\mu - \tau)$

......—— 3-fold Max. (vac.)

$E_\nu = 1.8 + E_e \ MeV \ \rightarrow$

Figure 6

Figure 7

LONG–BASELINE ${}^{(-)}_{e}$ APPEARANCE

$\cdots\cdots$ 3–fold Max. (vac.) $\Big\}$ $\Delta m^2 = 1.0 \; 10^{-3} \; eV^2$
──── 3–fold Max. (mat.)

2/9

$E_\nu = 1$ GeV

$E_\nu = 10$ GeV

$E_\nu = 100$ GeV

Figure 8